

Alma Mater Studiorum Università di Bologna  
Archivio istituzionale della ricerca

Power Line Interference Removal for High-Quality Continuous Biosignal Monitoring with Low-Power Wearable Devices

This is the final peer-reviewed author's accepted manuscript (postprint) of the following publication:

*Published Version:*

Tomasini, M., Benatti, S., Milosevic, B., Farella, E., Benini, L. (2016). Power Line Interference Removal for High-Quality Continuous Biosignal Monitoring with Low-Power Wearable Devices. IEEE SENSORS JOURNAL, 16(10), 3887-3895 [10.1109/JSEN.2016.2536363].

*Availability:*

This version is available at: <https://hdl.handle.net/11585/587107> since: 2019-03-26

*Published:*

DOI: <http://doi.org/10.1109/JSEN.2016.2536363>

*Terms of use:*

Some rights reserved. The terms and conditions for the reuse of this version of the manuscript are specified in the publishing policy. For all terms of use and more information see the publisher's website.

This item was downloaded from IRIS Università di Bologna (<https://cris.unibo.it/>).  
When citing, please refer to the published version.

(Article begins on next page)

This is the post peer-review accepted manuscript of:

M. Tomasini, S. Benatti, B. Milosevic, E. Farella and L. Benini "Power Line Interference Removal for High-Quality Continuous Biosignal Monitoring with Low-Power Wearable Devices," in IEEE SENSORS JOURNAL, vol. 16, no. 10, pp. 3887-3895, May 2016.

The published version is available online at:

<https://doi.org/10.1109/JSEN.2016.2536363>

© 2016 IEEE. Personal use of this material is permitted. Permission from IEEE must be obtained for all other uses, in any current or future media, including reprinting/republishing this material for advertising or promotional purposes, creating new collective works, for resale or redistribution to servers or lists, or reuse of any copyrighted component of this work in other works.

# Power Line Interference Removal for High Quality Continuous Bio-Signal Monitoring with low-power wearable devices

Marco Tomasini, Simone Benatti, *Student Member, IEEE*, Bojan Milosevic, Elisabetta Farella, *Member, IEEE*, and Luca Benini, *Fellow, IEEE*

**Abstract**—Mobile and long-term recording of biomedical signals such as ECG, EMG and EEG can improve diagnosis and monitor the evolution of several widespread diseases. However, it requires specific solutions, such as wearable devices that should be particularly comfortable for patients, while at the same time ensuring medical-grade signal acquisition quality, including Power Line Interference (PLI) removal. This work focuses on the on-board real-time PLI filtering on a low-power bio-potential acquisition wearable system. The paper analyzes in depth basic and advanced PLI filtering techniques and evaluates them in a wearable real-time processing scenario, assessing performance on EMG and ECG signals. Our experiments prove that most PLI removal algorithms are not usable in this challenging context, because they lack robustness or they require off-line processing and large amounts of available data. On the other hand, adaptive filtering techniques are robust and well-suited for lightweight on-line processing. We substantiate this finding with off-line analysis and comparison, as well as with a complete embedded implementation on our low-power low-cost wearable device.

**Keywords**—PLI removal, EMG, ECG, wearable computing, biomedical monitoring, sensor node

## I. INTRODUCTION

WEARABLE devices are becoming increasingly popular in several areas of modern healthcare practices, most notably in delivering point of care services, providing ambulatory monitoring within the healthcare environment and remote support for rehabilitating patients and the chronically ill at home. These devices act as supporting tools for doctors providing continuous assessment of critical physiological parameters or for identifying precursors of major adverse events [1]. They are also used in out-of-hospital environments to provide continuous monitoring solutions and real-time feedback information about the individual's health condition [2]–[5].

Wearable devices are capable of measuring significant physiological parameters, such as heart rate, blood pressure, body

and skin temperature, oxygen saturation, respiration rate, electrocardiogram, etc. Beside the data collection, further advantages are given by the development of smart devices, capable to process the acquired signals and run algorithms for the analysis of physiological parameters. This includes continuous collection and evaluation of multiple vital signs and intelligent multiparameter medical emergency detection. Therefore, it is necessary to provide low cost and low power wearable systems, equipped with sufficient computational resources to elaborate and analyze the biomedical signals in real-time with medical-grade quality [6].

Frequently used biopotentials, such as the Electrocardiogram (ECG) and the Electromyogram (EMG), lie in the  $1 \mu V - 10 mV$  range, with a bandwidth of  $0 - 1 kHz$ , while other biopotentials, such as the Electroneurogram (ENG), can reach a bandwidth of  $1 - 10 kHz$  [7]. Therefore, a correct acquisition of such signals requires an accurate design and a multilevel approach for noise reduction. Biomedical signals are often affected by interferences and artifacts, which may lead to their wrong interpretation. One major common source of interference is the Power Line Interference (PLI), which is due to the capacitive coupling between the subject and nearby electrical appliances and mains wiring [8]. The main frequency of the PLI is nominally at 50 Hz in Europe and 60 Hz in USA. However, it is non-stationary and frequency and amplitude variations are often detected and mainly originated from the AC power system. In particular, its frequency has variations of  $\pm 2 Hz$ , while the amplitude is heavily influenced by the system in use and the environment [9], [10].

Many solutions have been developed to reduce the interference in the acquired biomedical signals. Useful ways to reject the interferences include the use of active electrodes with integrated analog filters, the shielding and connection to ground of electrodes, subjects and nearby electrical appliances. In spite of these solutions, a significant residual interference remains. Moreover, the proposed solutions are often invasive and not suitable for wearable solutions.

Wearable sensor nodes are usually equipped with limited computational resources, thus the most common approach to reject the PLI from biomedical signals is the use of analog filters. This solution introduces non linear phase shifts, skewing the signal and it is costly in terms of component count and board space. Thus, additional signal processing techniques are necessary to filter the noise and achieve a robust output. The desired solution should remove the PLI even if it is

This work was supported in part by the EuroCPS EU Project under Grant 644090.

M. Tomasini, S. Benatti, and L. Benini are with the Department of Electrical, Electronic, and Information Engineering, University of Bologna, 40126 Bologna, Italy (e-mail: marco.tomasini@unibo.it; simone.benatti@unibo.it; luca.benini@unibo.it).

B. Milosevic and E. Farella are with the Energy Efficient Embedded Digital Architecture Unit, Fondazione Bruno Kessler, 38122 Trento, Italy (e-mail: milosevic@fbk.eu; efarella@fbk.eu).

L. Benini is with the Integrated Systems Laboratory, ETH Zurich, 8092 Zurich, Switzerland (e-mail: lbenini@iis.ee.ethz.ch).

non-stationary, while minimally affecting the frequency signal spectrum of interest. Furthermore, for a successful application in wearable solutions, it should be suitable for real-time implementation in resource constrained devices, requiring low computational complexity and low memory cost.

This paper analyzes the biopotential acquisition with a wearable platform [11] and evaluates its use for accurate real-time parameter monitoring with digital PLI filtering. We compared the four major classes of approaches for the PLI noise filtering, evaluating them with simulated signals and interference for an accurate study in a wide range of situations. Moreover, we implemented and profiled them on the embedded wearable platform evaluating accuracy and real-time performance. Based on this analysis, we demonstrate a highly effective PLI removal on our wearable smart platform in two applications: the acquisition of a 3-lead ECG, and the acquisition and processing of EMG signals.

## II. RELATED WORK

Several solutions for the removal of the PLI have been studied in the past decades. One of the approaches is the design of an analog front end with high Common Mode Rejection Ratio (CMRR). Hardware solutions have been developed to increase the actual CMRR by equalization of the cable shield and the use of a Driven Right Leg (DRL) circuit [12]. The DRL improves the CMRR by a closed loop compensation that provides a CM-canceling signal to the subject's body. This reduces the CM gain and boosts the CMRR, but it is affected by stability issues, which limit the effective improvement. The digitally-assisted DRL tunes the DRL loop's gain at the power line frequency, but needs an additional notch filter increasing power consumption. The common-mode feedback (CMFB) technique [13] improves CMRR by feeding the CM voltage back to the input of each pre-amplifier. The feedback loop is based on a summing amplifier and high value compensation capacitors to efficiently extract the CM noise. All these solutions require increased area, extra components and lead to an increased power consumption with a reduction of the common mode interference that is hardly higher than 40 dB [14].

For a more robust PLI removal, digital signal processing techniques are employed. The most common approach used to remove the PLI is a digital notch filter at the power line frequency (50 or 60 Hz) [15]–[17]. It has the advantage to be easily implemented and it has low computational requirements. However, the notch filter is not a good candidate to remove the PLI from biomedical signals with time-varying disturbances: to avoid signal distortion around the PLI frequency it needs a narrow notch frequency band, which leads to ineffective filtering when PLI frequency deviations are present.

A different approach is the time domain subtraction for PLI elimination [18]. This method first divides the signal in linear and non-linear segments by evaluating a threshold on its second derivative. In the linear segments, the signal is averaged and the PLI is estimated, which is then removed from both linear and non-linear segments. This approach is limited to the processing of ECG signals, which exhibit a periodic alternation between linear and non-linear segments. In fact, it

is not suitable for the denoising of EMG or EEG recordings since the linear and non linear segments in those cases cannot easily be identified in the presence of the PLI. Furthermore, the time domain subtraction alters considerably the spectrum for both lower and higher frequencies.

To overcome this limitation, newly developed techniques include the Sinusoidal Modeling (SM) [19] and Regression Subtraction (RS) [20], which accurately separate the PLI from biopotential signals. These methods share the same base approach, which consists in the estimation of the sinusoidal interference and its removal from the acquired signal. They estimate the amplitude and phase of the PLI and they reject the interference while minimally affecting the spectrum of the signal. On the other hand, these techniques lose their effectiveness when the frequency of the PLI is not constant and its deviation from the nominal value is not known. To overcome this drawback, it is necessary to calculate the Fast Fourier Transform (FFT) of the signal to localize with precision the value of the fundamental PLI frequency. This solution is not suitable for a real time implementation due the high computational cost to perform the FFT with adequate precision.

Another approach is the use of adaptive interference cancellation, which can track amplitude, phase and frequency of the PLI [21]. A drawback of this solution is that it requires a reference signal to estimate the frequency variations, which may not always be available in practice. To overcome this limitation, reference-free adaptive methods have been proposed in literature [22], [23]. Such methods are unfortunately sensitive to the ratio between the PLI and the signal amplitude in the interference frequency band. Therefore, they are not general and the parameters must be tuned case by case. An innovative adaptive filtering method was introduced by Keshtkaran et al. to track time fluctuations of the PLI's frequency, amplitude and phase [24], [25]. It can be used to process ECG, EEG and EMG signals without any reference signal, with the advantages of low computational complexity and low memory requirements, hence making it suitable for real time implementation in smart wearable solutions.

In recent years, there have been numerous research and commercial efforts in the design of wearable biopotentials measurement systems. One of the main challenges is to provide the device with adequate computational resources to execute signal processing on board, implementing a comfortable and feature rich solution, while providing adequate communication interface and battery life.

An example of a system for the monitoring of physiological signals is presented in [26]. This device is capable of achieving ubiquitous medical monitoring when interfaced to appropriate body worn sensors. The main limitation of the system is that the signal is filtered by an analog circuit due the insufficient computational resources of the wearable device. Another project presented in [27] is based on a PDA connected with a sensor board for ECG acquisition. The board is equipped with a two electrodes ECG amplifier, a MSP430 microprocessor and a Bluetooth Low Energy (BLE) radio module. This system is strongly oriented to a the ECG acquisition scenario, therefore there is a lack of flexibility.

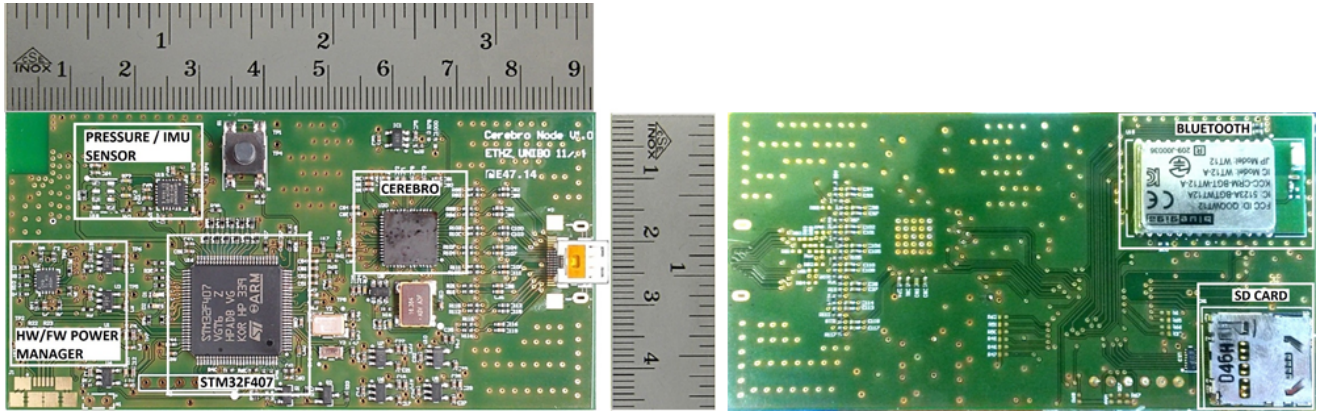


Fig. 1. Photograph of the top (left) and bottom (right) layers of the proposed device.

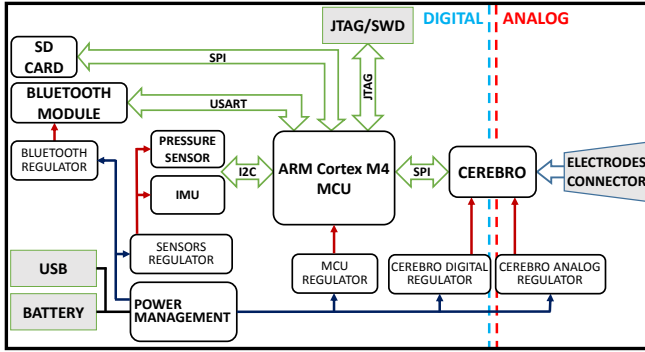


Fig. 2. Overview of the Cerebro wearable device.

Furthermore, it has only 2 channels, which is a limit to enable on board multimodal biosignals recording.

The lesson learned from existing approaches suggests that the design of a high-quality wearable device requires to couple an accurate AFE for the acquisition of biopotentials, with an efficient microcontroller (MCU) integrating DSP functionalities. This is the system architecture that we target in this study. It is in fact desirable for the AFE to integrate a digital backend for fast and reliable communication with the MCU, which must have sufficient computational resources to locally execute algorithms for filtering and information extraction to improve the quality of the signals.

### III. SYSTEM ARCHITECTURE

The presented wearable device pairs a high-performance and flexible AFE, well suited for the acquisition of the ECG, EMG and EEG signals, with an efficient MCU with integrated DSP functions. The PCB of the device is shown in Fig. 1, while the functional block diagram of the system is shown in Fig. 2.

The Cerebro AFE was designed for the use in low-power wearable devices for the acquisition of biopotential signals [20], [28], [29]. It is equipped with 8 differential AFE channels multiplexed to a shared 16 bit sigma-delta ADC, which samples each channel at up to 8kHz. This solution achieves a large CMRR (100dB) and an SNR of 95db, which is comparable

with commercial ICs for biopotential acquisition ADS1298 [30], BMD101 [31] and to state-of-the-art research solutions [32]. Moreover, Cerebro is equipped with an internal DAC used in a feedback loop to adjust the reference of each channel and remove any DC offset [33]. The platform is powered by an ARM Cortex M4 microcontroller (STM32F407) operating at a frequency of up to 168 MHz. The Cortex-M4 core is equipped with a single-precision hardware Floating point unit (FPU) and it implements a full set of DSP instructions. This architecture allows advanced and efficient digital processing capabilities, totaling 210 DMIPS (1.25 DMIPS/MHz). After the signals have been acquired and elaborated, they can be transmitted by a Bluetooth module to a nearby smartphone or they can be stored on a local SD card. Finally, additional inertial and pressure sensors have been added in order to collect data on the patient's motor activity.

To improve the energy efficiency of the device, the power supply of the board is handled by a dedicated power management circuitry, which automatically detects the power source in use (battery or USB connector). It manages the recharging of the battery, while providing low-dropout voltage regulators to the other submodels on board. This solution allows us to switch off the components of the board that are not necessary for a targeted biomedical application allowing the application of aggressive power saving strategies.

The board was designed with Altium Design CAD using 6 layers with 3 ground planes, 1 power plane and 2 signal layers. Discrete components are placed on both top and bottom layers in order to reduce the resulting size of the final system, which is  $91 \times 46$  mm. The board consumes 5mW for the reading and filtering of 4 bio-potential signals sampled at 1 kHz. It is powered by a 1350 mAh lithium-ion cell-phone battery, which lasts in the given configuration for more than 1 day of continuous signal recording.

### IV. PLI FILTERING METHODS

This section details the major digital filtering techniques and their parameters. In the rest of this paper, we denote:  $x_{sig}(n)$  as the true biomedical signal,  $p(n)$  as the PLI,  $x(n)$  as the contaminated signal and  $y(n)$  as the filtered output signal (see Fig. 3).

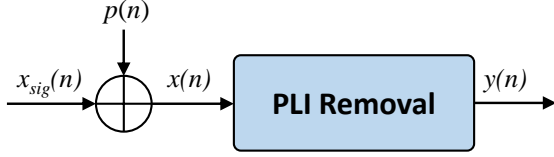


Fig. 3. Signal acquisition block diagram.

**Notch Filter.** The notch filter is a stop band filter that allows to attenuate component frequency in a narrow band. The transfer function of a real second order IIR filter is given in the following equation:

$$H(z) = \frac{Y(z)}{X(z)} = \frac{a_0 + a_1 z^{-1} + a_2 z^{-2}}{b_0 + b_1 z^{-1} + b_2 z^{-2}}$$

where  $a_0, a_1, a_2$  are the feed-forward and  $b_0, b_1, b_2$  are the feedback coefficients of the filter. The transfer function is implemented with the difference linear equation as follows:

$$a_0 y(n) = b_0 x(n) + b_1 x(n-1) + b_2 x(n-2) - a_1 y(n)(n-1) - a_2 y(n)(n-2)$$

In our implementation, we use a second order IIR filter centered at the PLI frequency with a bandwidth of 1Hz. In our experiments, the quality factor was set at 50 in order to reduce the PLI interference at approximately the same level of the ExG signal and thus avoid distortion of the bio-potentials in the frequency spectrum.

**Sinusoidal Modeling.** SM allows to remove the PLI and the baseline wander (BW) from the biomedical signal. This method models PLI and BW with a set of sinusoids modulated by low order time polynomials. It is expressed as follows:

$$p_{est}(t) = \sum_{i=0}^I (a_0^{(i)} + a_1^{(i)} t + a_2^{(i)} t^2) \sin(2\pi i f_{PLI} t) + (b_0^{(i)} + b_1^{(i)} t + b_2^{(i)} t^2) \cos(2\pi i f_{PLI} t)$$

where  $I$  is the total number of signal components in the model. The BW corresponds to the component with  $i = 0$ , while the PLI harmonics are modeled by the remaining ones ( $i \neq 0$ ). The sinusoids represent the harmonic character of the PLI signal with the fundamental frequency ( $i = 1$ ) corresponding to the PLI frequency ( $f_{PLI}$ ) in the analysis window. Moreover, the model is extended to include the DC component ( $i = 0$ ), whose time variations correspond to the BW signal component.

The coefficients of the model can be estimated by minimizing the quadratic error between the signal  $x(t)$  and the modeled PLI:

$$\min \left( \sum_{n=1}^N |x(t_n) - p_{est}(t_n)|^2 \right)$$

where  $t_n$  are the sampling instants in the analysis window. Finally, the estimated model is subtracted from the original signal to obtain a noise free signal  $y(t) = x(t) - p_{est}(t)$ .

We implemented this method to remove the first component of the power line interference ( $i = 1$ ) with  $f_{PLI} = 50\text{Hz}$

and a window size of  $1.5s$  as recommended in [19]. In our implementation, we do not include the DC component in the model, since Cerebro is equipped with an internal DAC used to adjust the reference of each channel and remove any DC offset [33]. The algorithm can be used in two modalities: in the first one, denoted as offline mode, the PLI is estimated and then subtracted from the same analysis window. In the second method, denoted as online mode, the PLI is estimated in one signal window and then it is subtracted from the subsequent window. The latter modality allows to use this approach in real-time applications.

**Regression Subtraction.** The acquired signal  $x_n = x_{sig}(n) + p(n)$  is the superposition of the biomedical signal  $x_{sig}(n)$  and the PLI components, modeled as:

$$p_i(n) = A_i \cdot \sin(2\pi \frac{f_{PLI,i}}{f_s} n + \varphi_i)$$

with amplitude  $A$ , phase  $\varphi$  and harmonic number  $i$ . This method considers a window of  $N$  samples multiple of  $(f_s/f_{PLI,i})$  where the phase and amplitude of the PLI are estimated in two steps. In the first step, in order to estimate  $\varphi_i$ , the algorithm projects the acquired sequence  $x(n)$  onto a locally generated cosine with known phase:

$$\frac{1}{N} \sum_{n=0}^{N-1} x(n) \cos(2\pi \frac{f_{PLI,i}}{f_s} n + \varphi_{est,i}) = \frac{1}{2} A_i \sin(\varphi_i - \varphi_{est,i})$$

Following, the method executes an iterative binary search to find the estimated phase  $\varphi_{est,i}$ . In the second step, the amplitude estimation ( $A_{est,i}$ ) is found by a projection onto an in-phase sinusoidal signal, as follows:

$$A_{est,i} = \frac{2}{N} \sum_{n=1}^{N-1} x(n) \sin(2\pi \frac{f_{PLI,i}}{f_s} n + \varphi_{est,i})$$

The estimated PLI noise is found using ( $A_{est,i}$ ) and ( $\varphi_{est,i}$ ) as follows:

$$p_{est,i}(n) = A_{est,i} \cdot \sin(2\pi \frac{f_{PLI,i}}{f_s} n + \varphi_{est,i})$$

Finally, the estimated noise is subtracted from the original signal to obtain a noise free signal. This method was implemented in software to remove the first component of the PLI, with  $f_{PLI} = 50\text{Hz}$  and a window size of  $1s$ . RS can also be applied in two modalities, online and offline, as described for SM.

**Adaptive PLI filter.** In our evaluation, we focus on the adaptive PLI filter (APF) proposed in [24] and [25], due to its capability to process heterogeneous vital signs and their low computational and memory requirements. This approach iteratively estimates the fundamental frequency of the PLI and then generates its other harmonics. At each sample, the estimated PLI is subtracted from the noise-affected biosignal in order to reject the PLI. The APF distinguishes two methods for the estimation of amplitude and phase of the interference: in APF LMS the amplitude and phase of each harmonic are obtained using a least mean square algorithm, while the



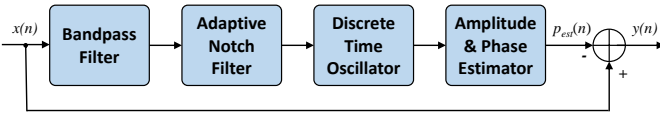


Fig. 4. Block diagram of the adaptive PLI filter.

APF RLS uses a simplified recursive least squares algorithm to approximate the PLI parameters. Beside the parameter estimation algorithm, the two APF approaches are equal.

Fig. 4 shows the functional blocks of the APF algorithm. The bandpass filter is used to preprocess the signal to enhance the fundamental harmonic of the PLI and to obtain a robust estimation of its frequency. This filter is also useful for the attenuation of lower frequency artifacts and signal components, which may negatively affect the frequency estimation. If the nominal power line frequency is known to be at 50 Hz, the bandpass filter can be set to 45-55Hz, but it can be further customized to accommodate both 50Hz and 60Hz powerline frequencies. The next stage consists in an Adaptive Notch Filter (ANF) for frequency estimation. It is implemented through a lattice algorithm [34] to obtain high performance in the instantaneous estimation of the PLI frequency with low complexity and suitability for real-time finite precision implementation. Next, the discrete-time oscillators and the amplitude phase estimator are used to generate the estimated PLI sinusoid. Defining the estimation error as  $e(n) = x(n) - p_{est}(n)$ , the APF LMS method minimizes the cost function:

$$E(n) = \mathbb{E}|e(n)|^2$$

while the APF RLS minimizes the cost function:

$$E(n) = \sum_{n=1}^{N-1} \lambda_a^{(N-1-n)} e^2(n)$$

In this case,  $\lambda_a$  is the forgetting factor and  $0 \ll \lambda_a < 1$ . Finally, the estimated interference  $p_{est}(n)$  is subtracted from the input signal  $x(n)$  to obtain a noise-free signal  $y(n)$ . In our experiments, we tested both approaches to remove the first component of the PLI and we followed the guidelines presented in [24] for a correct adjustment of the parameters in each block.

## V. EXPERIMENTAL RESULTS

In this section, we present an extensive analysis using off-line ECG data and simulated PLI to quantitatively evaluate the methods under various signals and parameters conditions. Furthermore, the algorithms were all implemented on the microcontroller of our wearable device and they were tested on real-time acquisition and filtering of ECG and EMG signals.

### A. Off-line analysis setup

To analyze the characteristics of the aforementioned algorithms under various signal conditions, we used ECG data taken from the PTB Diagnostic ECG Database, which is part of the Pysionet project [35]. The biopotentials are sampled at 1 kHz with 16-bit resolution over a  $\pm 16.384 mV$  range

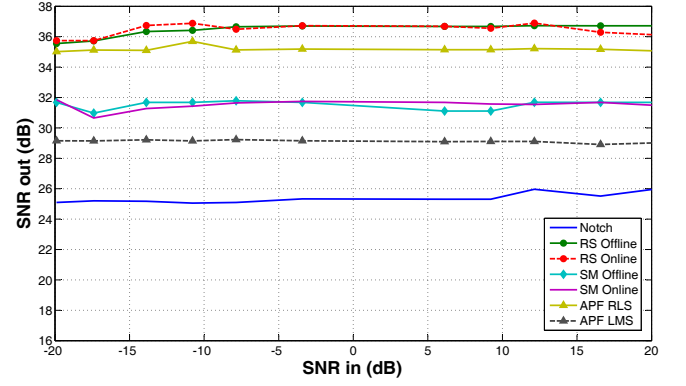


Fig. 5. Sensitivity to PLI amplitude.

and have variable duration (from 30s to 2min). In each test, we added a synthetic PLI containing 1 harmonic to the ECG signal, with variable frequency and amplitude as specified in each simulation. To denote the signal to noise ratios (SNRs) of the input and output signals we used  $SNR_{IN}$  and  $SNR_{OUT}$ , defined as:

$$SNR_{IN} = 20 \log_{10} \frac{\|x_{sig}\|_2}{\|p\|_2}$$

$$SNR_{OUT} = 20 \log_{10} \frac{\|y\|_2}{\|x_{sig} - y\|_2}$$

### B. Sensitivity to Power Line Amplitude

To achieve a proper interference cancellation, the algorithm should work robustly under several  $SNR_{IN}$  conditions. To evaluate this feature, we simulated signal sequences whose  $SNR_{IN}$  ranged from -20dB to 20dB. For each  $SNR_{IN}$  value, we added a 50Hz sinusoidal interference to the signal and each method was applied to remove such interference, computing the resulting  $SNR_{OUT}$ . Figure 5 shows the  $SNR_{OUT}$  for each  $SNR_{IN}$  at the sampling rate of 1 kHz.

In this test, executed with a constant PLI frequency, we can observe that both online and offline modalities reach the same performance in removing the PLI for all  $SNR_{IN}$  values. In fact, high values of  $SNR_{OUT}$  are noticed for both RS (36dB) and SM (31dB) approaches. The APF RLS and APF LMS achieve a constant  $SNR_{OUT}$  of 35dB and 29dB respectively, indicating that the performance of the APF methods is robust with respect to  $SNR_{IN}$ . The notch filter demonstrates to be the worst method in this comparison, with  $SNR_{OUT} = 25dB$ .

### C. Sensitivity to Power Line Frequency Variability

In real life scenarios, the frequency of the PLI is not constant at exactly 50Hz, hence it is important to evaluate the performance of these techniques with regard to PLI frequency variations. The notch filter, SM and RS, all need to know a priori the fundamental frequency of the interference ( $f_{PLI}$ ). On the other hand, the APF approach can automatically detect

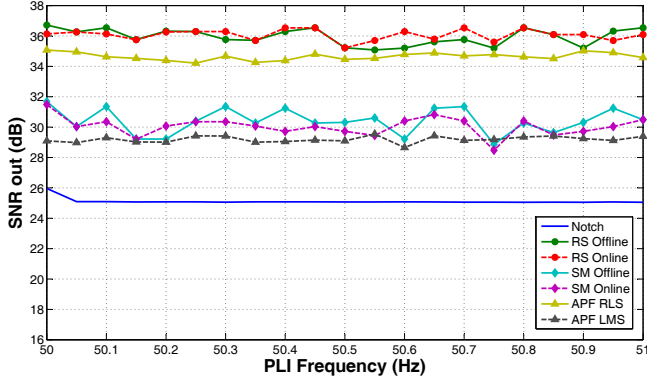


Fig. 6. Sensitivity to power line frequency variations when  $f_{PLI}$  is known.

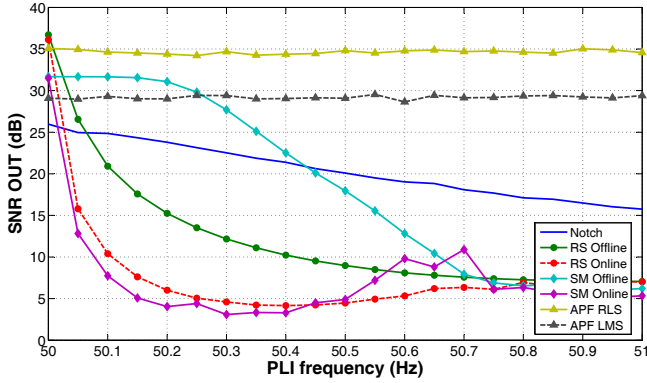


Fig. 7. Sensitivity to power line frequency variations when  $f_{PLI}$  is unknown.

the value of the frequency interference and no a priori setting of its nominal value is required.

To test the capabilities of the algorithms to remove the PLI under varying powerline frequencies, we used as the input of each method synthetic sequences with  $SNR_{IN}$  equal to 6dB and PLI frequency ranging between 50 and 51 Hz. We computed the output SNRs to evaluate the performance of the algorithms. In this test, we assumed to know a priori the frequency value of the powerline interference and set  $f_{PLI}$  correctly in each trial. Figure 6 shows the  $SNR_{OUT}$  achieved by each method. We can observe that SM, RS and APF, all achieve a  $SNR_{OUT}$  of up to 29dB. The notch filter is again the worst method, with  $SNR_{OUT} = 25dB$ .

The accurate value of the PLI is unknown in a real scenario, and may also change over time, thus it is important to test the performance of the algorithms when  $f_{PLI}$  is not known. Hence, we performed the same experiment as described before, but with  $f_{PLI}$  always set to 50 Hz. Figure 7 shows the resultant  $SNR_{OUT}$ . Here, we can observe that for a frequency deviation smaller than 0.01Hz the notch filter, SM online and RS (online and offline) correctly remove the PLI from the biomedical signals, with  $SNR_{OUT} > 30dB$ . For a frequency deviation higher than 0.01Hz, all these algorithms lose their effectiveness. In fact, we can observe an  $SNR_{OUT}$  lower than 30dB for all of them. SM offline is adequately robust to achieve an  $SNR_{OUT}$  of up to 30dB only for frequency deviations lower than 0.3Hz. Moreover, the performance of

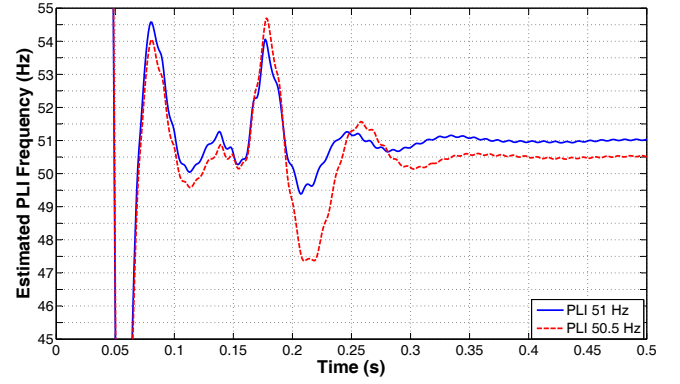


Fig. 8. Convergence behavior of the APF.

SM and RS online deteriorates rapidly if the number of samples in a window used to estimate the interference is not an exact multiple of the number of samples in a PLI period. In the non-multiple sampling case there is a variance of the initial PLI phase between two consecutive windows, therefore the PLI estimated in one signal window and then subtracted from the subsequent window is not correctly aligned. The notch filter, on the other side, shows a lower but slowly declining  $SNR_{OUT}$ , hence resulting more robust to frequency deviations. The best performance is achieved with the APF approaches, in particular the APF RLS shows high values of  $SNR_{OUT} (\geq 35dB)$  consistently achieved for varying PLI frequencies deviations.

SM and RS algorithms need an accurate estimate of the  $f_{PLI}$  to achieve good results. The frequency of the interference is estimated by computing the FFT of the input signal and localizing the strongest bin in the 45 - 55 Hz range. As resulted from experimental analysis, high performance is achieved when the estimate is accurate with a resolution of 0.01Hz. The number of samples required to achieve such resolution depends on the signal's sampling period. When sampling at 1kHz, we need 100000 samples, which implies that we have to wait more than 1 minute to collect data for a PLI frequency estimate at the required level of resolution. This automatically rules out the use of these algorithms for real-time continuous monitoring: not only the FFT would be very demanding in terms of computation and storage, but also the PLI frequency can fluctuate significantly during the 1 minute interval, thereby fundamentally limiting the achievable accuracy.

In contrast, the APF methods can effectively track the variations in the PLI frequency. To demonstrate the fast convergence of this approach, two synthetic sequences with main frequencies of 50.5Hz and 51Hz were tested. In Figure 8 we can observe the frequency convergence of the APF RLS, where the frequency estimates converge to the actual fundamental frequency (i.e. 50.5Hz and 51Hz) in less than 400ms, while maintaining an  $SNR_{OUT}$  of 35db.

#### D. Evaluation on the Cerebro platform

To demonstrate the capabilities of our system and to evaluate the performance of the algorithms in a real-life application scenario, we collected ECG and EMG signals with the Cerebro



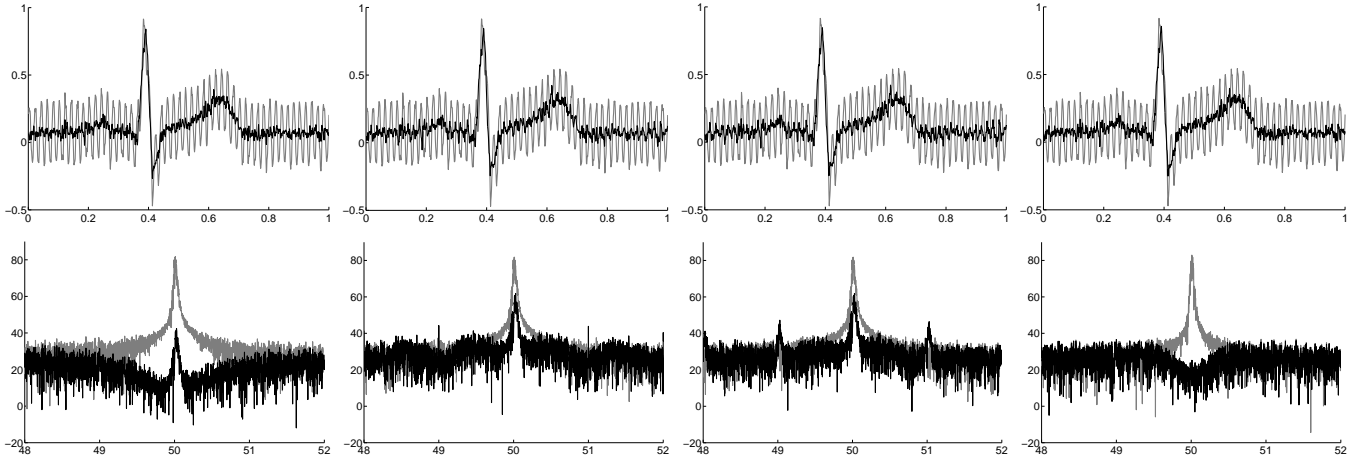


Fig. 9. PLI removal for ECG signals. Top row: raw and filtered signals (units: seconds and mV), bottom row: frequency spectrum (units: Hz and dB); from left to right: notch, SM, RS, APF.

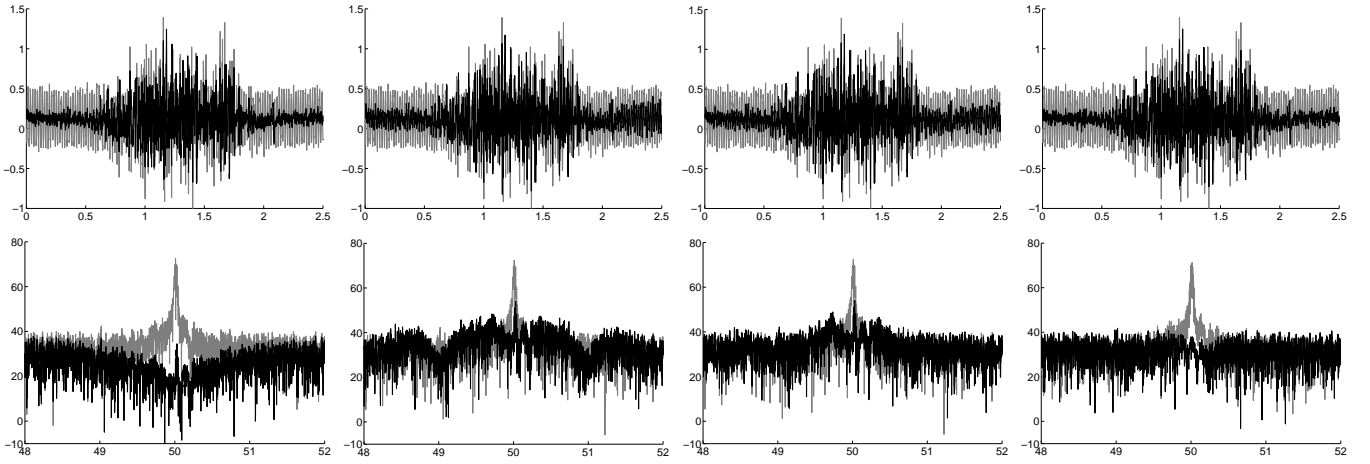


Fig. 10. PLI removal for EMG signals. Top row: raw and filtered signals (units: seconds and mV), bottom row: frequency spectrum (units: Hz and dB); from left to right: notch, SM, RS, APF.

platform. Data was collected from three subjects with acquisitions of up to 10 min. The signals were sampled at 1kHz with a gain of 32.

For the ECG, we used a 3-lead acquisition setup, where one differential channel of Cerebro was used to acquire the signal. We placed two disposable electrodes on the wrists of the user and an additional electrode was placed on the right ankle as the reference potential. The EMG signal was acquired with one differential pair of electrodes placed on the forearm of the subjects and an additional electrode was placed on the elbow as the reference potential. Using the data acquired with Cerebro, we compared the filtering performance of the considered algorithms, evaluating the online versions of the RS and SM algorithms and the RLS version of the APF, which outperforms the LMS one. The Cerebro platform was shown to be capable of acquiring high quality biopotential signals in controlled environments [29]. To fully exploit its wearable nature, we compared the proposed PLI filtering techniques evaluating their effects on the frequency spectrum and computational costs. In this case, we do not have an exact

computation of  $SNR_{OUT}$ , since we do not have  $p(t)$ , but we can compare the frequency spectrum of original and filtered signals.

The result of the PLI removal from the ECG and EMG signal is shown in Fig. 9 and 10, where we plotted the raw and the filtered signals along with their frequency spectrum. Ideally, the perfect filtering technique should remove the PLI component and leave the rest of the signal spectrum unchanged. The visual difference in the filtered signals is minimal, but from the spectrum plots we can note that the notch filter, RS online and SM online fail to adequately remove the interference. The notch filter removes also frequency components close the PLI, while the RS and SM present minimal alterations of the surrounding frequency spectrum, but they do not completely remove the PLI. The APF RLS delivers considerably better signal quality, indeed it is very precise to remove the PLI without additional changes in the signal's spectrum.

Finally, we evaluated the computational cost of the algorithms. For the SM and RS approaches we calculated the computational cost to filter the signal in a window of  $N$  samples

TABLE I. COMPUTATIONAL AND MEMORY REQUIREMENTS.

Algorithm	Computational Cost (ms)	Memory (byte)
Notch	0.002	48 byte
Sinusoidal Modeling	79	84040
Regression Subtraction	8.3	8160
APF RLS	0.036	184

equal to 1500 (1.5s) and 1000 (1s) respectively. The notch and APF are iterative approaches applied at each new sample. Computational and memory costs are summarized in Table I. Here we can note that the APF has the lowest computational cost, requiring only  $36\mu s$  at each sample, making it a preferred choice for real-time implementation. The notch filter is also characterized by a low computational cost, but it introduces distortion in the signal, therefore it is not a good candidate to remove the PLI from biomedical signals. SM and RS are much more demanding with respectively 79ms and 8.3ms needed to process each window. Moreover, they have considerably higher memory requirements and they do not perform as well as the APF RLS in the continuous monitoring scenario characterized by frequency fluctuations of the PLI signal.

## VI. CONCLUSION

In this paper, we presented the evaluation of PLI filtering techniques for a wearable device, targeting their on-board implementation and considering platforms with adequate processing capabilities to acquire high quality heterogeneous biopotential signals. In particular, we considered the acquisition of EMG and ECG signals and we described the implementation and performance of four main PLI removal methods. For quantitative and qualitative analysis of their characteristics, we performed extensive simulation using real ECG data and simulated interference with various signal conditions. The different approaches were also implemented and profiled on the embedded wearable system, evaluating them in terms of accuracy to reject the PLI and real-time performance. In particular, we demonstrate that the APF RLS takes only a few hundreds of milliseconds to autonomously tune its parameters and converge to the input PLI frequency, while the other approaches need several minutes for accurate frequency estimation. Furthermore, APF RLS has the best performance in terms of output SNR and it best preserves the frequency characteristics of the targeted signals, while having minimal computational cost.

## ACKNOWLEDGMENT

This work was partially funded by the Nano-Tera.ch ICYSoC project, which is financed by the Swiss Confederation and scientifically evaluated by SNSF. It was also funded by the EuroCPS EU project (GA 644090).

## REFERENCES

- [1] R. Bushko, *Future of Intelligent and Extelligent Health Environment*. IOS Press, 2005.
- [2] A. Pantelopoulou and N. Bourbakis, "A survey on wearable sensor-based systems for health monitoring and prognosis," *Systems, Man, and Cybernetics, Part C: Applications and Reviews, IEEE Transactions on*, vol. 40, no. 1, pp. 1–12, Jan 2010.
- [3] I. Korhonen, J. Parkka, and M. van Gils, "Health monitoring in the home of the future," *Engineering in Medicine and Biology Magazine, IEEE*, vol. 22, no. 3, pp. 66–73, May 2003.
- [4] C. Wong, Z.-Q. Zhang, B. Lo, and G.-Z. Yang, "Wearable sensing for solid biomechanics: A review," *Sensors Journal, IEEE*, vol. 15, no. 5, pp. 2747–2760, May 2015.
- [5] S. Mukhopadhyay, "Wearable sensors for human activity monitoring: A review," *Sensors Journal, IEEE*, vol. 15, no. 3, pp. 1321–1330, March 2015.
- [6] M. Rodgers, V. Pai, and R. Conroy, "Recent advances in wearable sensors for health monitoring," *Sensors Journal, IEEE*, vol. 15, no. 6, pp. 3119–3126, June 2015.
- [7] R. Rangayyan, *Biomedical Signal Analysis*, ser. IEEE Press Series on Biomedical Engineering. Wiley, 2015.
- [8] M. Chimene and R. Pallas-Areny, "A comprehensive model for power line interference in biopotential measurements," *Instrumentation and Measurement, IEEE Transactions on*, vol. 49, no. 3, pp. 535–540, Jun 2000.
- [9] C. D. McManus, K.-D. Neubert, and E. Cramer, "Characterization and elimination of AC noise in electrocardiograms: A comparison of digital filtering methods," *Computers and Biomedical Research*, vol. 26, no. 1, pp. 48 – 67, 1993.
- [10] R. C. Dugan, M. F. McGranaghan, S. Santoso, and H. W. Beaty, *Electrical power systems quality*. McGraw-Hill, 2003.
- [11] S. Benatti, F. Casamassima, B. Milosevic, E. Farella, P. Schonle, S. Fateh, T. Burger, Q. Huang, and L. Benini, "A versatile embedded platform for EMG acquisition and gesture recognition," *Biomedical Circuits and Systems, IEEE Transactions on*, vol. 9, no. 5, pp. 620–630, Oct 2015.
- [12] A. Metting van Rijn, A. Peper, and C. Grimbergen, "High-quality recording of bioelectric events," *Medical and Biological Engineering and Computing*, vol. 28, no. 5, pp. 389–397, 1990.
- [13] J. Xu, R. Yazicioglu, B. Grundelheuer, P. Harpe, K. Makinwa, and C. Van Hoof, "A 160uW 8-channel active electrode system for EEG monitoring," *Biomedical Circuits and Systems, IEEE Transactions on*, vol. 5, no. 6, pp. 555–567, Dec 2011.
- [14] M. Haberman and E. Spinelli, "A multichannel EEG acquisition scheme based on single ended amplifiers and digital DRL," *Biomedical Circuits and Systems, IEEE Transactions on*, vol. 6, no. 6, pp. 614–618, Dec 2012.
- [15] K. Hirano, S. Nishimura, and S. Mitra, "Design of digital notch filters," *Communications, IEEE Transactions on*, vol. 22, no. 7, pp. 964–970, Jul 1974.
- [16] S.-C. Pei and C.-C. Tseng, "Elimination of AC interference in electrocardiogram using IIR notch filter with transient suppression," *Biomedical Engineering, IEEE Transactions on*, vol. 42, no. 11, pp. 1128–1132, Nov 1995.
- [17] J. Piskorowski, "Digital Q-Varying Notch IIR Filter With Transient Suppression," *Instrumentation and Measurement, IEEE Transactions on*, vol. 59, no. 4, pp. 866–872, April 2010.
- [18] C. Levkov, G. Mihov, R. Ivanov, I. Daskalov, I. Christov, and I. Dotsinsky, "Removal of power-line interference from the ECG: a review of the subtraction procedure," *BioMedical Engineering OnLine*, vol. 4, no. 1, p. 50, 2005.
- [19] M. Zivanovic and M. Gonzalez-Izal, "Simultaneous powerline interference and baseline wander removal from ECG and EMG signals by sinusoidal modeling," *Medical Engineering & Physics*, vol. 35, no. 10, pp. 1431 – 1441, 2013.
- [20] P. Schonle, F. Schulthess, S. Fateh, R. Ulrich, F. Huang, T. Burger, and Q. Huang, "A dc-connectable multi-channel biomedical data acquisition

asic with mains frequency cancellation,” in *ESSCIRC (ESSCIRC), 2013 Proceedings of the*, Sept 2013, pp. 149–152.

- [21] B. Widrow, J. Glover, J.R., J. McCool, J. Kaunitz, C. Williams, R. Hearn, J. Zeidler, J. Eugene Dong, and R. Goodlin, “Adaptive noise cancelling: Principles and applications,” *Proceedings of the IEEE*, vol. 63, no. 12, pp. 1692–1716, Dec 1975.
- [22] A. Ziarani and A. Konrad, “A nonlinear adaptive method of elimination of power line interference in ECG signals,” *Biomedical Engineering, IEEE Transactions on*, vol. 49, no. 6, pp. 540–547, June 2002.
- [23] S. Martens, M. Mischi, S. Oei, and J. Bergmans, “An improved adaptive power line interference canceller for electrocardiography,” *Biomedical Engineering, IEEE Transactions on*, vol. 53, no. 11, pp. 2220–2231, Nov 2006.
- [24] M. R. Keshtkaran and Z. Yang, “A fast, robust algorithm for power line interference cancellation in neural recording,” *Journal of Neural Engineering*, vol. 11, no. 2, 2014.
- [25] M. Keshtkaran and Z. Yang, “A Robust Adaptive Power Line Interference Canceller VLSI Architecture and ASIC for Multichannel Biopotential Recording Applications,” *Circuits and Systems II: Express Briefs, IEEE Transactions on*, vol. 61, no. 10, pp. 788–792, 2014.
- [26] A.-W. Wong, D. McDonagh, G. Kathiresan, O. Omeni, O. El-Jamaly, T.-K. Chan, P. Paddan, and A. Burdett, “A 1V, Micropower System-on-Chip for Vital-Sign Monitoring in Wireless Body Sensor Networks,” in *Solid-State Circuits Conference, 2008. ISSCC 2008. Digest of Technical Papers. IEEE International*, Feb 2008, pp. 138–602.
- [27] E. Prawiro, C.-C. Hu, Y.-S. Chan, C.-H. Chang, and Y.-H. Lin, “A heart rate detection method for low power exercise intensity monitoring device,” in *Bioelectronics and Bioinformatics (ISBB), 2014 IEEE International Symposium on*, April 2014, pp. 1–4.
- [28] S. Benatti, B. Milosevic, F. Casamassima, P. Schonle, P. Bunjaku, S. Fateh, Q. Huang, and L. Benini, “Emg-based hand gesture recognition with flexible analog front end,” in *Biomedical Circuits and Systems Conference (BioCAS), 2014 IEEE*, Oct 2014, pp. 57–60.
- [29] S. Benatti, B. Milosevic, M. Tomasini, E. Farella, P. Schönle, P. Bunjaku, G. Rovere, S. Fateh, and L. Huang, Q. and Benini, “Multiple biopotentials acquisition system for wearable applications,” in *Biomedical Engineering Systems and Technologies Conference (BIOSTEC), 2015 INSTICC*, Jan 2015.
- [30] Texas Instrumets ADS1298, <http://www.ti.com/product/ADS1298>, [online, retrieved on 15/12/2015].
- [31] NeuroSky BMD101, <http://store.neurosky.com/products/ecg-bmd101>, [online, retrieved on 15/12/2015].
- [32] N. Van Helleputte, M. Konijnenburg, J. Pettine, D.-W. Jee, H. Kim, A. Morgado, R. Van Wegberg, T. Torfs, R. Mohan, A. Breeschoten, H. de Groot, C. Van Hoof, and R. Yazicioglu, “A 345 uW Multi-Sensor Biomedical SoC With Bio-Impedance, 3-Channel ECG, Motion Artifact Reduction, and Integrated DSP,” *Solid-State Circuits, IEEE Journal of*, vol. 50, no. 1, pp. 230–244, Jan 2015.
- [33] M. Tomasini, S. Benatti, F. Casamassima, B. Milosevic, S. Fateh, E. Farella, and L. Benini, “Digitally controlled feedback for DC offset cancellation in a wearable multichannel EMG platform,” in *Intl. Conf. of the IEEE Engineering in Medicine and Biology Society (EMBC). IEEE*, 2015, pp. 3189–3192.
- [34] N. Cho and S. Lee, “On the adaptive lattice notch filter for the detection of sinusoids,” *Circuits and Systems II: Analog and Digital Signal Processing, IEEE Transactions on*, vol. 40, no. 7, pp. 405–416, Jul 1993.
- [35] A. L. Goldberger, L. A. N. Amaral, L. Glass, J. M. Hausdorff, P. C. Ivanov, R. G. Mark, J. E. Mietus, G. B. Moody, C.-K. Peng, and H. E. Stanley, “Physiobank, physiotoolkit, and physionet: Components of a new research resource for complex physiologic signals,” *Circulation*, vol. 101, no. 23, pp. e215–e220, Jun 2000.



**Marco Tomasini** Recieved the M.Sc. in Automation Engineering from the University of Bologna in 2014. In 2015 he joined the Micrel Lab at the University of Bologna where he received a scholarship under the supervision of Prof. Luca Benini. His main research topic is wearable devices for biomedical applications. His scientific interests are analog front end, sensor fusion, signal processing.



sensor fusion and actuation systems.

**Simone Benatti** (S'15) Recieved the M.Sc. in Electrical Engineering from the University of Bologna in 2004. From 2005 to 2012 he worked as HW/FW designer for a biomedical company. In 2012 he joined the Micrel Lab at the University of Bologna where he enrolled as a PhD student under the supervision of Prof. Luca Benini. In 2015 he was at UC Berkeley as a visiting scholar. His main research topics are on embedded systems, EMG-based gesture recognition, prosthetics and BMI. His scientific interests are in embedded wearable system, signal processing, sensor fusion and actuation systems.



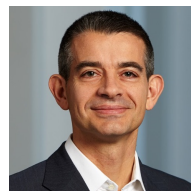
in the same lab, he is from 2014 a researcher at the Fondazione Bruno Kessler (FBK) in Trento, Italy, within the E3DA Unit.

**Bojan Milosevic** Recieved the B.Sc. and M.Sc. degrees in elctrical engineering from the University of Bologna in 2006 and 2009 respectively. In 2010 he joined the Micrel Lab at the same university where he enrolled as a PhD student under the supervision of Prof. Luca Benini and in 2012 he recieved the Intel Doctoral Award. He got his PhD degree in 2013 with a thesis on the hardware and software development of efficient embedded systems with applications in ambient intelligence, healthcare and human machine interaction. After one year as a post-doc researcher in the same lab, he is from 2014 a researcher at the Fondazione Bruno Kessler (FBK) in Trento, Italy, within the E3DA Unit.



3D human-computer interaction. She worked since 2014 as coordinator of the research activities on body sensor and actuators networks, smart objects and tangible interfaces at the Department of Electrical, Electronic and Information Engineering (DEI) at University of Bologna within the group of Prof. Luca Benini.

**Elisabetta Farella** (M'14) Elisabetta Farella is head of the research unit E3DA - Energy Efficient Embedded Digital Architecture at ICT center FBK from 2014. She received a Ph.D degree in electrical engineering and computer science from University of Ferrara in March 2005. Her research activity is in the field of microelectronics, with particular reference to components, systems and their application, mainly in the following fields: Wireless Sensor Networks, Ambient Intelligence, Wearable Electronics (for health and rehabilitation), Internet-of-Things for natural and



**Luca Benini** (F'07) is Full Professor at the University of Bologna and he is the chair of Digital Circuits and Systems at ETHZ. Dr. Benini's research interests are in energy-efficient system design and Multi-Core SoC design. He is also active in the area of energy-efficient smart sensors and sensor networks for biomedical and ambient intelligence applications. He has published more than 700 papers in peer-reviewed international journals and conferences, four books and several book chapters. He is a member of the Academia Europaea.